Remarks on the black hole shadows in Kerr-de Sitter space times.

Eunice Omwoyo, Humberto Belich, Júlio C. Fabris,Hermano Velten

PPGCosmo-Universidade Federal do Espírito Santo

Agenda

Black holes are regions of very strong gravity that is sufficient to warp space, bend light and give rise to space-time singularities.

It is most probable that all black holes in nature are rotating and are therefore described by the Kerr solution.

In the presence of a cosmological constant, a generalization of the Kerr metric is given by the Kerr-de Sitter metric.

Recently, a new solution has been proposed, the Kerr-de Sitter Revisited solution.

Due to the presence of the cosmological constant, these space times have four horizons.

For astrophysical processes, another radius associated with cosmic repulsion is relevant the so-called static radius.

When a black hole is in front of a luminous background, its unstable photon region, a region containing null geodesics at a constant radius, will be projected on the observer's sky to form the so-called black hole shadow.

A set of coordinates must be established in order to locate the shadow in the sky. These coordinates are referred to as the celestial coordinates.

Celestial coordinates can be calculated for distant observers or for observers at arbitrary distance form the black hole.

In Kerr de Sitter space time, the celestial coordinates have always been obtained for observers at arbitrary distances. This is due to the space time being asymptotically de sitter.

What is the intent of this work?

In this work, we intend to study the black hole shadows of Kerr de Sitter space times for observers specifically located in the vicinity of the static radius.

What is special about the static radius?

On the static radius boundary, gravitational attraction due to the central compact object and cosmic repulsion counterbalance each other.

By the use of embedding diagrams it has been shown that in the vicinity of the static radius, the geometry of de Sitter space-time is analogous to an asymptotically flat space-time.

Thus, in this work, we make use of this property (treating the vicinity of the static radius as an analogue of asymptotically flat) and fix our observers in this vicinity.

Kerr de Sitter space time

In Boyer-Lindquist coordinates $(t, r, \ , \ )$, the Kerr-de Sitter Metric is given by

$$ds^2 = \frac{a^2 \quad \sin^2(\ )}{L^2} \quad \frac{r}{L^2} \quad dt^2 \quad \frac{2a\sin^2(\ ) \quad a^2 + r^2 \quad r}{L^2} dtd$$
$$+ \frac{\sin^2(\ ) \quad a^2 + r^2 \ ^2 \quad a^2 \quad r\sin^2(\ )}{L^2} d \ ^2 + \frac{}{} d \ ^2 + \frac{}{r} dr^2; \quad (1)$$

where the terms appearing in the metric coefficients are defined as,

$$= \quad 1 + \frac{a^2\cos^2}{3}; \quad (2)$$

$$_r \quad = \quad (1 \quad \frac{r^2}{3})(r^2 + a^2) \quad 2Mr; \quad (3)$$

$$L \quad = \quad 1 + \frac{a^2}{3}; \quad (4)$$

$$= \quad r^2 + a^2\cos^2 \ : \quad (5)$$

Kerr de Sitter space time

The metric does not depend on t and hence possesses two killing vectors.

Roots of $_r$ yields the horizons of this space time. This parameter is a quartic polynomial, hence there are four roots.

Kerr de Sitter space time

Geodesics in KdS space time.

The necessary geodesics for the study of black hole shadows are null geodesics. The null geodesics in KdS space time are given as,

$$\overline{E}p^{r} = \sqrt{R(r)}; \tag{6}$$

$$\overline{E}p = \sqrt{\quad(\quad)}; \tag{7}$$

$$\overline{E}p = \frac{aL^{2}}{r}(a(a \quad) + r^{2}) \quad \frac{L^{2}}{\sin^{2}}(a\sin^{2} \quad); \tag{8}$$

$$\overline{E}p^{t} = \frac{L^{2}}{r}((r^{2}+a^{2})^{2} \quad a\ (a^{2}+r^{2})) \quad \frac{aL^{2}}{}(a\sin^{2} \quad): \tag{9}$$

Where,

$$R(r) = L^{2}(r^{2}+a^{2} \quad a\ )^{2} \quad {}_{r}(\ +L^{2}(\quad a)^{2}); \tag{10}$$

$$(\ ) = a^{2} \quad L^{2} + a^{2}L^{2}\cos^{2}(\ ) \quad a^{2}L^{2} \quad 2a \quad L^{2} + 2a\ L^{2} + \quad + \quad {}^{2}L^{2} \quad {}^{2}L^{2}\cot \tag{11}$$

Kerr de Sitter space time

The special case of null geodesics

The critical curve of the black hole shadow is formed null geodesics at a constant radius., i.e spherical photon orbits.

How can spherical photon orbits be obtained?

$$R(r) = 0; \quad R^{0}(r) = 0; \tag{12}$$

This condition yields,

$$= \frac{L^2 r^3 \quad 6a^2 \quad r^2(3M + r) \quad 6M \quad + a^4 \quad ^2 r^3 + 9r(r \quad 3M)^2}{a^2 \left(r \left(a^2 \quad + 2 \quad r^2 \quad 3\right) + 3M\right)^2}; \tag{13}$$

$$= \frac{r \quad a^2 \quad 6 \quad r^2 \quad + 3r(r \quad 3M)}{a \left(r \left(a^2 \quad + 2 \quad r^2 \quad 3\right) + 3M\right)} + a: \tag{14}$$

These two parameters are the constants of motion governing the motion of spherical photon orbits.

Kerr de Sitter space time

How does govern the motion of spherical photon orbits?

When > 0, the orbits move above and below the equatorial plane. At = 0, they are confined on the equatorial plane, forming the equatorial circular prograde and retrograde orbits.

Figura 1: A null geodesic at a constant radius.

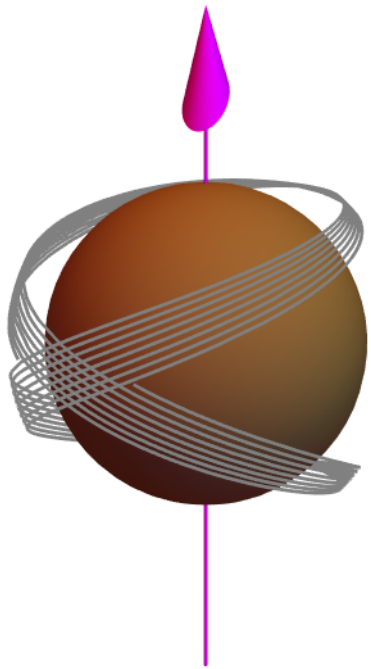

Kerr de Sitter space time

Thus, solving for r when $\quad = 0$ results in,

$$r_{ph+;KdS} = \frac{2M(y \quad 1)}{(y+1)^2} + 2\sqrt{\frac{M^2((y \quad 14)y+1)}{(y+1)^4}}\cos\left(\frac{\quad}{3}\right) + \frac{4}{3} \quad ; \qquad (15)$$

$$r_{ph \quad ;KdS} = \frac{2M(y \quad 1)}{(y+1)^2} + 2\sqrt{\frac{M^2((y \quad 14)y+1)}{(y+1)^4}}\cos\left(\frac{\quad}{3}\right) \quad : \qquad (16)$$

$r_{ph+;KdS}$ forms the lower bound while $r_{ph \quad ;KdS}$ forms the upper bound of the photon orbits at a constant radius. Thus the KdS photon region is the region with $r \ 2 \ [r_{ph+;KdS}; r_{ph \quad ;KdS}]$.

Kerr de Sitter Revisited space time

The Kerr-de Sitter revisited solution is defined by the metric,

$$ds^2 = \frac{a^2 \sin^2}{2} dt^2 + \frac{2}{} dr^2 + {}^2 d\ {}^2 + \frac{\sin^2}{2} d\ {}^2$$

$$\frac{2a \sin^2}{2} (r^2 + a^2 \quad) dtd \ ; \quad (17)$$

with,

$$= r^2 \quad 2Mr + a^2 \quad \frac{r^4}{3}; \quad (18)$$

$$= (r^2 + a^2)^2 \quad a^2 \sin^2 \ ; \quad (19)$$

$$^2 = r^2 + a^2 \cos^2 \ : \quad (20)$$

Two killing vectors and horizons.

Kerr de Sitter Revisited space time

We obtain the null geodesics as,

$$\frac{}{E}^{2} p^{r} = \quad \sqrt{\quad} R\ (r); \tag{21}$$

$$\frac{}{E}^{2} p = \quad \sqrt{\quad} (\ ); \tag{22}$$

$$\frac{}{E}^{2} p = \frac{(ar^2 + a^3 \quad a \qquad a^2 \quad)}{} + \frac{}{\sin^2}; \tag{23}$$

$$\frac{}{E}^{2} p^{t} = \frac{(r^2 + a^2)(r^2 + a^2 \quad a \quad)}{} + a \qquad a^2 \sin^2 \ ; \tag{24}$$

where,

$$R\ (r) = (r^2 + a^2 \quad a \quad)^2 \qquad (\quad + (\qquad a)^2); \tag{25}$$

$$(\ ) = \quad + a^2 \cos^2 \qquad ^2 \cot^2 \ : \tag{26}$$

Kerr de Sitter Revisited space time

Using the condition for spherical photon orbits, $R\ (r) = R^{0}(r) = 0$, we obtain,

$$= \frac{3r^3\ \ 4a^2\ \ r^3\ \ 3M\ \ + 3r(r\ \ 3M)^2}{a^2(3M\ +\ 2\ \ r^3\ \ 3r)^2}; \tag{27}$$

$$= \frac{3a^2M\ +\ 2a^2\ \ r^3\ +\ 3a^2r\ \ 9Mr^2\ +\ 3r^3}{a(3M\ +\ 2\ \ r^3\ \ 3r)}: \tag{28}$$

and are still constants of motion governing spherical photon orbits. Thus the roots of will yield the radii of equatorial circular prograde and retrograde photon orbits.

Kerr de Sitter Revisited space time

Solving for r in $\quad = 0$,

$$r_{ph+;RKdS} = \frac{6M}{4a^2 \quad + 3} + 6 \sqrt{\frac{M^2(1 \quad 4a^2 \quad)}{(4a^2 \quad + 3)^2}} \cos \quad \frac{\sim}{3} + \frac{4}{3} \quad ; \qquad (29)$$

$$r_{ph \quad ;RKdS} = \frac{6M}{4a^2 \quad + 3} + 6 \sqrt{\frac{M^2(1 \quad 4a^2 \quad)}{(4a^2 \quad + 3)^2}} \cos \quad \frac{\sim}{3} \quad : \qquad (30)$$

Thus, the photon region in Kerr de Sitter Revisited space time exists in $r \quad 2$ $[r_{ph+;RKdS}; r_{ph \quad ;RKdS}]$

Celestial Coordinates

KdS

$$_{KdS} = \frac{p\overline{3L^2}\sin(\ )\ a\qquad \csc^2(\ )}{L^2(a^2\qquad 2a\quad +\ ^2\ +3)+}; \tag{31}$$

$$_{KdS} = \frac{p\overline{3}(\quad p\frac{}{(\ ))}}{L^2(a^2\qquad 2a\quad +\ ^2\ +3)+}; \tag{32}$$

RKdS

$$_{RKdS} = \frac{p\overline{3}\csc(\ )(a\cos(2\ )\quad a+2\ \ )}{2\ \ a^2\qquad 2a\quad +\quad +\ ^2\ +3}; \tag{33}$$

$$_{RKdS} = \frac{p\overline{3}\ q\frac{}{a^2\cos^2(\ )+\qquad ^2\cot^2(\ )}}{a^2\qquad 2a\quad +\quad +\ ^2\ +3}: \tag{34}$$

Celestial Coordinates

How do we test that the celestial coordinates are correct?

Since the shadow is formed by the projection of the photon region on the observers sky, then the critical curve of the shadow should exhibit the behaviour of the corresponding spherical photon orbits.

Figura 2: Critical curve of the black hole shadow.

Celestial Coordinates

Figura 3: Radius of Equatorial circular Prograde orbit, KdS

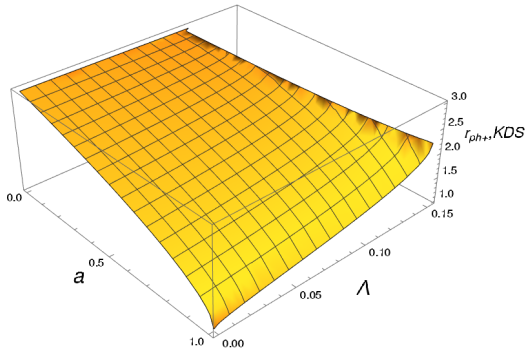

Figura 4: Radius of Equatorial circular Prograde orbit, RKdS

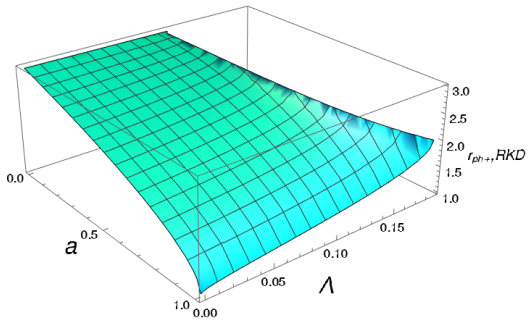

Celestial Coordinates

Figura 5: KdS black hole shadows for different values of a

Figura 6: RKdS black hole shadows for different values of a

Celestial Coordinates

Figura 7: Radius of Equatorial circular Retrograde orbit, KdS

Figura 8: Radius of Equatorial circular Retrograde orbit, RKdS

Celestial Coordinates

Figura 9: KdS black hole shadows for different

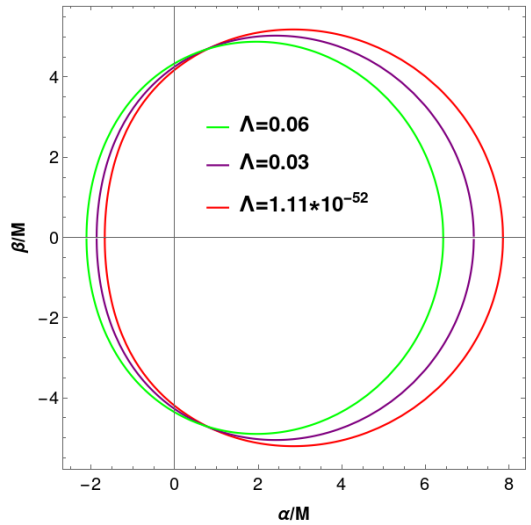

Figura 10: RKdS black hole shadows for different

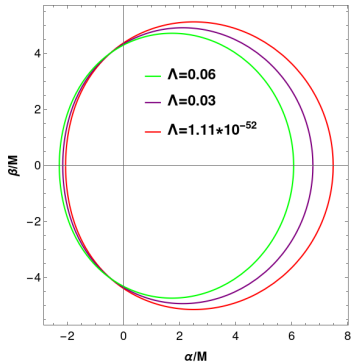

Quantitative Analysis of the shadows

Radius of curvature

$$R_{curvature} = \frac{(\ {}^{0}(r)^2 + \ {}^{0}(r)^2)^{3=2}}{{}^{0}(r)\ {}^{00}(r) \qquad {}^{0}(r)\ {}^{00}(r)} : \tag{35}$$

Figura 11: Points at which we calculate the radius of curvature

Quantitative Analysis of the shadows

Tabela 1: Points evaluated for = 16 , a = 0:5 and = 1:11 $\times$ 10 ^{52}m ^{2}

points	Kerr	kds	rkds
(as)	38.9617	38.9617	38.9617
(as)	38.9123	38.9123	38.9123
R_T(as)	19.4318	19.4318	19.4318
R_D(as)	19.5096	19.5099	19.5099
R_R(as)	19.502	19.502	19.502

.

We model our values to M87

For this value of , the values are indistinguishable.

Quantitative Analysis of the shadows

Tabela 2: Points evaluated for = 16 , a = 0:5 and = 0:06m ^{2}

points	kds, (31,32)	rkds, (33,34)
(as)	38.6587	38.3582
(as)	38.6533	38.267
R_T(as)	19.2878	19.0882
R_D(as)	19.4078	19.2278
R_R(as)	19.4021	19.2221

For this value of , the values are distinguishable, however note that this value is not astrophysically relevant.

Qualitative Analysis of the shadows

Recently, the 2017 Event Horizon Telescope observations of M87 were utilized and a constraint on the characteristic areal radius of the shadow was obtained.

It was shown that the radius of the shadow must lie in the range [4.31M, 6.08M].

We used this constraint on the shadow to constrain the black hole spin and angle of inclination of our observer.

Qualitative Analysis of the shadows

Figura 12: Excluded and permitted regions for a shadow cast by a Kerr-de Sitter black hole.

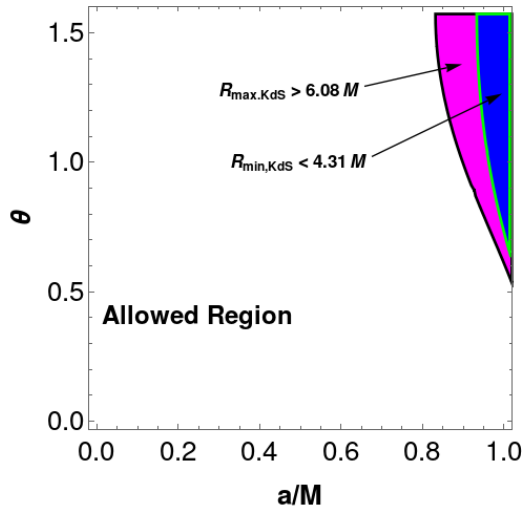

Figura 13: Excluded and permitted regions for a shadow cast by a Kerr-de Sitter Revisited black hole.

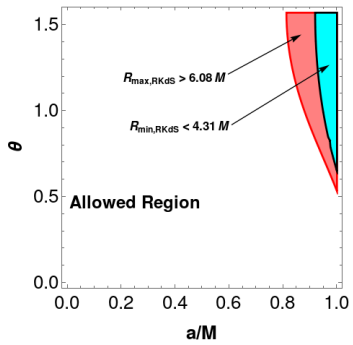

Qualitative Analysis of the shadows

We observe that in both black holes, excluded regions appear at high black hole spin $a/M > 0{:}812311$ and larger angles of inclination $> 0{:}532512 \quad 30{:}5107$.

for small angles of inclination, no excluded regions occur.

Thus, for a KdS and RKdS black hole, small angles of inclination pass the constraints of M87* observations.

Conclusion

We have analyzed black hole shadows in Kerr-de Sitter and Kerr-de Sitter Revisited space-times for observers located in the vicinity of the static radius.

We have investigated their qualitative and quantitative behavior.

For astrophysically relevant observations (= 1:11 10 $^{52}m^2$), a Kerr, Kerr-de Sitter and Kerr-de Sitter Revisited black hole shadow cannot be distinguished.

Finally, utilizing the constraint on the characteristic areal radius of the shadow obtained by the Event Horizon Telescope collaboration, we have constrained a Kerr-de Sitter and a Kerr-de Sitter Revisited black hole.

We nd that, for $a/M > 0{:}812311$, large angles of inclination $> 0{:}532512$ $30{:}5107$ are excluded from M87* observations in both Kerr-de Sitter and a Kerr-de Sitter Revisited black hole.